

Evaluation of the impact of surfactants on miscibility of griseofulvin in spray dried amorphous solid dispersions

Article

Accepted Version

Bhanderi, A., Bari, F. and Al-Obaidi, H. ORCID:
<https://orcid.org/0000-0001-9735-0303> (2021) Evaluation of the impact of surfactants on miscibility of griseofulvin in spray dried amorphous solid dispersions. *Journal of Drug Delivery Science and Technology*, 64. 102606. ISSN 1773-2247 doi:
<https://doi.org/10.1016/j.jddst.2021.102606> Available at
<https://centaur.reading.ac.uk/98743/>

It is advisable to refer to the publisher's version if you intend to cite from the work. See [Guidance on citing](#).

To link to this article DOI: <http://dx.doi.org/10.1016/j.jddst.2021.102606>

Publisher: Elsevier

All outputs in CentAUR are protected by Intellectual Property Rights law, including copyright law. Copyright and IPR is retained by the creators or other copyright holders. Terms and conditions for use of this material are defined in the [End User Agreement](#).

www.reading.ac.uk/centaur

CentAUR

Central Archive at the University of Reading

Reading's research outputs online

1 **Evaluation of the impact of surfactants on miscibility of**
2 **griseofulvin in spray dried amorphous solid dispersions**

3 Amit Bhanderi, Fiza Bari, Hisham Al-Obaidi*

4 *The School of Pharmacy, University of Reading, Reading RG6 6AD, UK*

5
6
7
8
9
10
11
12
13
14
15
16
17
18
19
20
21
22
23
24
25
26
27
28
29
30
31
32
33
34
35
36
37
38
39
40

The School of Pharmacy

University of Reading

Whiteknights, PO Box 226

RG6 6AP

Reading, UK

T: +44 118 378 6261

h.al-obaidi@reading.ac.uk

Keywords: Amorphous solid dispersions, surfactants, miscibility, solubility, glass transition temperature,
Flory-Huggins

41 **Abstract**

42 The aim of this contribution is to examine the impact of incorporating surfactants into
43 amorphous solid dispersions on solid state miscibility and aqueous solubility of the antifungal
44 drug griseofulvin. Spray dried amorphous solid dispersions of griseofulvin (GF) and
45 hypromellose acetate succinate (HPMCAS) were prepared by spray drying. Three different
46 surfactants of varying ratios between 1 to 5% were used namely the anionic sodium dodecyl
47 sulfate (SDS), the cationic dodecyletrimethylammonium bromide (DTAB) and the non-ionic
48 pluronic (F127). Flory-Huggins model combined with calculations based on Hoffman's equation
49 were used to calculate miscibility and predicted solubility of the amorphous form. The results
50 showed that the prepared solid dispersions exhibited enhanced drug-polymer miscibility
51 reflected by improved thermodynamics of mixing. The highest miscibility was achieved when
52 DTAB was incorporated by which the drug-polymer miscibility was enhanced by approximately
53 1.5 times. The tendency to recrystallize was calculated using reduced recrystallization
54 parameter and correlated with the measured saturation solubility showing distinct properties
55 which were dependent on the type of surfactant. Saturated solubility of the solid dispersions
56 was compared with micellar solubility and was found to be significantly affected by the presence
57 of the polymer. The glass transition temperature (T_g) decreased significantly upon the addition
58 of surfactants. However, gravimetric analysis showed that solvent content did not exceed 1%
59 which suggests that the shifted T_g was not related to plasticizing effect of residual solvent.
60 Overall, these results suggest potential role for the surfactants in enhancing solid state
61 miscibility when incorporated into the solid dispersions.

62

63

64 **Introduction**

65 Converting crystalline drugs to the amorphous form has been accepted as effective approach to
66 improve solubility of hydrophobic drugs [1-3]. The favourable amorphous form has a higher
67 energy manifesting in higher apparent solubility and enhanced dissolution rates compared to
68 the crystalline form of the drug [4, 5]. Formation of amorphous solid dispersions has been
69 commonly used to formulate amorphous drugs. However, the amorphous form is
70 thermodynamically unstable and tend to re-crystallize over a period of time [6]. Recrystallization
71 can occur during storage (solid-state-mediated) or after administration of the drug (solution-
72 mediated), or both. Use of solid dispersions in which the drug is molecularly mixed with a
73 hydrophilic polymer has been successful in preventing recrystallization of the amorphous drug
74 [7].

75 One potential event that can be difficult to predict is whether the drug would remain amorphous
76 upon exposure to the aqueous medium. This is particularly difficult to measure for fragile glass
77 formers because of their high tendency to recrystallize [8]. We have shown before that a
78 memory exists in solid particles where properties (such as formed H-bonds) in the solid state
79 remained even after the drug has completely dissolved [9]. Hence it is possible to maintain
80 drug-polymer interactions so that to improve the solubility of the poorly soluble drug. The latter
81 can be achieved via enhancing drug-polymer solid state miscibility. Apart from amorphous form
82 formation, incorporation of surfactants in the solid dispersion can be used as additional method
83 to improve solubility. Previous studies have shown that anionic surfactants had a significant
84 effect on the binding of GF to the polymer polyethylene glycol [10]. This was attributed to
85 counterions forming a bridge between the polymer causing the aggregation of anionic surfactant
86 and GF. This effect will not be seen with a non-ionic surfactant and will be smaller for cationic
87 surfactants. The impact of the counterion on the properties of the dispersion has been studied
88 and was shown to vary according to the charge to radius ratio [11]. For example, compared to
89 K^+ and Na^+ , Li^+ has a larger charge/radius causing it to exhibit greater binding ability between
90 the polymer and the drug; therefore Li^+ counterions have greater impact on the properties of the
91 dispersion [11].

92

93 In a more recent study, the anionic surfactant sodium dodecyl sulfate (SDS) was shown to
94 enhance nucleation of hesperetin crystals but equally slowing down crystal growth [12]. There
95 are other studies in the literature which have investigated the impact of surfactants on the
96 interactions of drug and polymer in solid dispersions. For example, impact of crystallization of
97 itraconazole was studied in solid dispersions that included sodium lauryl sulfate and d- α -
98 tocopheryl polyethylene glycol 1000 succinate. The authors showed that sodium lauryl sulfate/
99 Soluplus[®] improved solid state stability and solubility of itraconazole [13]. In a different study,
100 surfactants were found to interfere with the crystallization inhibitory efficiency of the polymers in
101 spray dried amorphous solid dispersions [13].

102 Despite previous research, we believe that the impact of surfactants on induction/inhibition of
103 recrystallization of amorphous drugs is still not well understood. This stems from our previous
104 work in which we have shown that surfactants displayed different behaviour in terms of their
105 impact on drug polymer miscibility depending on the method of preparation [14]. Here in this
106 work, we use thermal analysis to measure the impact of surfactants on solid state miscibility of
107 the drug and the polymer. This approach is based on measuring configurational energy of the
108 amorphous form and calculate solubility ratio (amorphous/crystalline). We compare the results

109 with predictions made using Flory-Huggins model based on analysing physical mixtures of the
110 drug/polymer/surfactant. The prepared amorphous solid dispersions contain griseofulvin (GF)
111 as the model drug which is known to exhibit low aqueous solubility while the polymer is
112 hypromellose acetate succinate (HPMCAS). Three different surfactants were selected to be
113 incorporated into the amorphous solid dispersions of GF/ HPMCAS which are the anionic
114 sodium dodecyl sulfate (SDS), the cationic dodecyletrimethylammonium bromide (DTAB) and
115 the non-ionic pluronic (F127) (Figure 1). The rationale for selecting those surfactants is based
116 on that SDS and DTAB have similar length of carbon chain (12 carbons) with relatively
117 comparable critical micellar concentration (CMC). Pluronic F127 is a non-ionic surfactant and
118 was selected to compare the impact of charge existence on the interaction with GF and acidic
119 HPMCAS. In addition, these surfactants vary in terms of the critical micellar concentration
120 (CMC) exhibiting a range between 0.3 to 15 mM [15-17]. This variation in the CMC provides
121 additional factor for comparing the impact on solubility and the possible involvement of micellar
122 solubilization in polymer-surfactants interactions. The mass ratio of the surfactants was varied
123 between 1 to 5% so that to cover a range of concentrations across the CMC. These surfactants
124 are commonly used excipients for pharmaceutical applications hence there is a need to
125 understand their impact on drug-polymer interactions.

126

127 **Figure 1:** The chemical structures of griseofulvin, HPMCAS and surfactants.

128

129 **Experimental section**

130 **Materials**

131 GF was purchased from Sigma-Aldrich (Dorset, UK) and HPMCAS obtained from Shin-Etsu
132 chemical (Tokyo, Japan). Sodium dodecyl sulfate (SDS, 99% purity),
133 Dodecyletrimethylammonium bromide (DTAB, $\geq 98\%$ purity) and pluronic (F127) were obtained
134 from Sigma- Aldrich (Dorset, UK). Acetone and NaOH pellets were purchased from VWR
135 International LTD (UK), and sodium dihydrogen orthophosphate purchased from Fisher Scientific
136 (Loughborough, UK). All chemicals were used without further purification.

137

138 **Preparation of Physical Mixtures**

139 Physical mixtures of varying GF:HPMCAS weight ratios which weighed a total of 1g were
140 prepared by the method of trituration using a pestle and mortar for 10 minutes (Table 1). The first
141 set of physical mixtures acted as the control for the study containing no added surfactant. The
142 remainder of the physical mixtures were made up using the same ratios and took into account the

143 added surfactant SDS (1%, 2.5% and 5%) and Pluronic F-127 (1%, 2.5% and 5%) and DTAB
144 (1%, 2.5% and 5%).

145

146 The size of the particles (physical mixtures) was controlled using sieving so that a narrow particle
147 size distribution was chosen (40-90 μm). This step is necessary to conduct DSC studies that
148 were needed for the application of the Flory-Huggins model. Thus, the onsets of the melting
149 peaks obtained from DSC measurements correspond to the interaction between the API and the
150 polymer rather than due to different particles sizes of the physical mixtures.

151

152 **Preparation of GF-HPMCAS and GF-HPMCAS-surfactants solid dispersions**

153 Binary solid dispersions consisting of GF and HPMCAS were prepared at mass ratio 50% GF.
154 The total amount of dispersion produced was 5 g by which 2.5 g of GF was added to a 500 mL
155 conical flask with 185 mL of acetone. The mixture was then stirred for 10 minutes until the GF
156 had completely dissolved. 85 mL of distilled water was added to the conical flask and the solution
157 was then stirred for further 10 minutes, followed by addition of 2.5 g of HPMCAS. The final mixture
158 was then stirred for approximately 45 mins until the mixture was completely clear. The solution
159 was finally spray dried to produce the solid dispersion of drug and polymer, using Niro SD-Micro
160 spray dryer (Søborg, Denmark). This was connected to a nitrogen generator (Gateshead, UK),
161 where the nitrogen gas was used as the chamber and atomizer gas. Parameters which were set
162 for spray-drying were: inlet pressure temperature of 65°C, outlet temperature of 45°C, chamber
163 gas flow of 25 kg/h, atomizer gas (nitrogen) flow of 2.5 kg/h, and a fixed nozzle diameter of 0.5
164 mm.

165 For preparing GF-HPMCAS-surfactants solid dispersions, different amounts of surfactants were
166 used to prepare dispersions with fixed amounts of GF and HPMCAS of 50% each. 1, 2.5 and 5%
167 of each surfactant was used to prepare these dispersions with 50% GF and 50% HPMCAS. The
168 same procedure was carried out for each percentage of surfactant, for SDS, DTAB and F127.
169 Similar spray drying conditions were used to prepare the GF-HPMCAS-surfactants. The outlet
170 temperature was significantly below the T_g of the particles hence the impact of preparation method
171 on crystallization was minimal.

172

173 **Thermal analysis of prepared solid dispersions**

174 Differential scanning calorimetry (DSC) was conducted on the prepared solid dispersions, which
175 consisted of GF-HPMCAS and GF-HPMCAS- surfactants, using DSC 2920 Modulates DSC (TA
176 instrument, UK). 5-10 mg of samples were accurately weighed into an aluminium pan, and then

177 hermitically crimped. The method used to measure the glass transition temperature of solid
178 dispersions were set at a heating rate of 10°C/min using 20mL/min N₂ purge gas, and using empty
179 pan as the reference. Indium was used as a calibrant which measured an onset melting point of
180 156.6°C.

181

182

183

184 **Measurement of melting point depression of physical mixtures**

185 5-10 mg of a sample of each physical mixture containing GF and HPMCAS alone and those which
186 contained surfactants were weighed accurately in an aluminium pan and hermitically sealed. The
187 method used to measure the onset of melting was first to equilibrate at 80°C, then keep it
188 isothermal for 10 minutes, and finally to ramp at 5°C/min to 245°C, with an empty pan used as a
189 reference. All measurements were done in triplicates and the average and standard deviation
190 values were calculated.

191

192 **Saturation solubility measurements**

193 Accurately weighed samples which contained amount equivalent to 5 mg of GF were added to
194 microcentrifuge tubes. 1 mL of phosphate buffer solution (pH 6.8) was added into each of the
195 microcentrifuge tubes. The tubes were then placed on a Stuart® SB2 mechanical mixer
196 (Staffordshire, UK) for 72 hours. The tubes were centrifuged using Heraeus Biofuge Pico
197 (Germany) at 13,000 rpm for 10 minutes. The supernatant was then separated to measure
198 absorbance using Elmer Perkins UV spectrophotometer (Cambridgeshire, UK) at 295 nm.

199

200 **Thermogravimetric analysis (TGA)**

201 Residual solvent content was analysed using a Perkin Elmer thermogravimetric analyzer TGA 6
202 with Pyris 6 TGA software (Perkin Elmer Corporation). Nitrogen was used as the purge gas at
203 20 mL/min, and each sample was heated at 10°C/min from 20°C to 200°C. All measurements
204 were repeated in triplicates and the average and standard deviation values were calculated.

205

206 **Fourier Transform Infrared (FTIR)**

207 Infrared spectra were obtained from a Nicolet Nextus 470 FTIR spectrometer, Thermo Electron
208 Corporation (Massachusetts, USA) which was equipped with a KBr beam splitter. An attenuated
209 total reflectance accessory was used to obtain the spectra, in the form of a single reflection

210 bounce diamond crystal, Golden Gate accessory). A total of 64 scans were collected for each
211 sample with a resolution of 4 cm^{-1} using a frequency range of 4000 cm^{-1} to 550 cm^{-1} .

212

213 **Measurement of particle size distribution**

214 The size distribution of particles in the physical mixtures and solid dispersions was assessed
215 using Malvern Mastersizer (Worcestershire, UK). Phosphate buffer solution (pH 6.8) was used to
216 disperse the particles. Ten consecutive repeat measurements were carried out, each with 2500
217 sweeps and an interference of 20%.

218

219 **Scanning Electron Microscopy (SEM)**

220 The sample particles were fixed on to the surface of a conductive double-sided carbon adhesive,
221 attached to an aluminium stub. The prepared samples were sputter coated with gold, for 3 minutes
222 at 30 mA, using Emitech K550 (Ashford, UK). The micrographs were collected using a Philips FEI
223 KL (Eindhoven, Netherlands).

224

225 **Statistical analysis**

226 Statistical analysis of the data was carried out by one-way analysis of variance (ANOVA) with
227 Tukey's multiple comparison tests at a significance level of $p < 0.05$ using SPSS 22 software
228 (IBM).

229

230 **Results**

231 **Glass transition temperature and thermogravimetric analysis**

232 The glass transition temperature (T_g) is a second order transition event that occurs when the
233 amorphous glassy state changes to the less viscous supercooled liquid. The non-equilibrium
234 nature of glassy state will encourage higher molecular mobility leading to relaxation and loss of
235 excess configurational energy. The impact of adding the surfactants was evaluated by
236 measuring the T_g of the solid dispersions. Lowering in the T_g was observed when the
237 surfactants were incorporated into the solid dispersions. As can be seen in Figure 2, the T_g
238 values have been reduced significantly when surfactants were added into the solid dispersions
239 with maximum lowering was observed when F127 was incorporated. Insignificant statistical
240 difference between different ratios was observed for dispersions containing SDS. A statistical
241 difference was only seen for dispersions containing 5% DTAB compared with the 1 and 2.5%
242 while all ratios of F127 showed significant difference. The average T_g values were significantly
243 different between F127 and SDS/DTAB while there was no statistical difference between the

244 average T_g values for DTAB and SDS dispersions. One possible explanation for the significant
245 reduction in the T_g is the presence of residual solvents. Hence, to examine this effect,
246 thermogravimetric analysis (TGA) was performed.

247

248 **Figure 2:** (a) Typical DSC thermogram showing different thermal events when heating GF:
249 HPMCAS solid dispersions and (b) glass transition temperature values (T_g) for spray dried
250 amorphous solid dispersions prepared using GF: HPMCAS (50%:50%) containing different
251 ratios of the surfactants (SDS, DTAB, F127). The dotted line shows the T_g for the GF/HPMCAS
252 amorphous solid dispersion without surfactants.

253

254 As can be seen in Table 2, the amount of residual solvent did not differ significantly between the
255 various solid dispersions with an average residual solvent content of around 1%. Hence, the
256 lower T_g values could not be attributed to the presence of solvent but rather due to the effect of
257 the surfactant on the drug-polymer matrix.

258

259

260 **Measurement of melting point (T_m) and heat of fusion of physical mixtures and prediction** 261 **of thermodynamics of mixing**

262 Figure 3 shows the onset of melting peak and heat of fusion of physical mixtures. As can be
263 seen, overall trend showed reduction in both melting point onset and heat of fusion. There were
264 differences in the extent of this lowering by which SDS containing mixtures were associated
265 with the sharpest decline in the melting point followed by DTAB whilst minor differences were
266 observed for mixtures that contained F127 compared to mixtures without surfactants. The heat
267 of fusion which represents the total enthalpy of the crystalline lattice did not follow the same
268 trend by which F127 mixtures showed the sharpest reduction compared to other mixtures. It is
269 worth mentioning that shifts in thermal events often reflects good miscibility between the drug
270 and the polymer. These can also happen when non uniform crystalline domains form during
271 recrystallization. On the other hand, there are examples in the literature where no differences in
272 terms of the melting point depression could be observed [18]. Due to thermal degradation of
273 some mixtures, measurement of the heat of fusion was not possible.

274

275 **Figure 3:** (a) onset of melting point of GF in physical mixtures of GF: HPMCAS containing
276 varied ratios of the surfactants and (b) heat of fusion of the physical mixtures. Some physical
277 mixtures such as SDS mixtures were not possible to measure due to thermal degradation.

278

279 Flory-Huggins model was used to analyse the shifts in the heat of fusion and melting point
280 depression of physical mixtures. This modified model takes into account the molecular volume
281 of the drug in relation to the polymer. The polymer is theoretically divided into voids that are
282 equivalent to the molecular volume of the drug. Hence, the incidence of interactions between
283 the polymer and the drug are normalized thus the smaller the molecular volume (and therefore
284 the voids) of the drug, the highest is the entropy effect. This positive impact on free energy of
285 mixing is counterbalanced by the enthalpy of mixing which is accounted for through the Flory-
286 Huggins interaction parameter (χ). Using thermal analysis of drug-polymer physical mixtures,
287 this parameter can be calculated using both depression in the melting point as well as the molar
288 heat of fusion. Despite some drawbacks associated with the use of this method, it can provide
289 significant insight on the extent of interactions especially when similar systems are compared.

290

291 For the determination of enthalpy, entropy and energy of mixing, the Flory-Huggins model was
292 applied [18-20]. ΔG_M is the free energy of mixing for n_{drug} and $n_{polymer}$, present at Φ_{drug} and $\Phi_{polymer}$
293 volume fractions. The interaction parameter χ accounts for the enthalpy of mixing. It can be
294 calculated from equation (1) and then substituted into (2) to find the free energy of mixing [18,
295 19].

296

$$\frac{\Delta G_M}{RT} = n_{drug} \ln \Phi_{drug} + n_{polymer} \ln \Phi_{polymer} + \chi n_{drug} \Phi_{polymer}$$

(1)

299

$$\left(\frac{1}{T_M^{mix}} - \frac{1}{T_M^{pure}} \right) = \frac{-R}{\Delta H_{fus}} \left[\ln \Phi_{drug} + \left(1 - \frac{1}{m} \right) \Phi_{polymer} + \chi \Phi_{polymer}^2 \right]$$

(2)

302

303 where T_M^{mix} and T_M^{pure} are the melting temperatures of the drug in the presence of polymer and
304 alone, respectively; ΔH_{fus} is the enthalpy of fusion of pure drug, and m is the ratio of the polymer
305 to drug volume (calculated as molar volumes derived from true density).

306

307 As can be seen in Figure 4, the results showed that physical mixtures that contained DTAB
308 were associated with the lowest free energy of mixing compared to other mixtures. Thermal
309 degradation was more pronounced in SDS containing mixtures hence only 1% mixtures were
310 analysed. There was obvious difference in the extent of mixing by which the surfactants lowered

311 the free energy of mixing and ultimately means the miscibility of the drug and the polymer are
312 enhanced. Consequently, the drug-polymer miscibility was enhanced by approximately 1.3
313 folds when 2.5% DTAB was incorporated. This approximation is based on free energy of mixing
314 for mixtures without surfactants of -3.1×10^{-6} J/g which was lowered to -4.4×10^{-5} J/g for DTAB
315 mixtures. Due to thermal degradation, mixtures that contained higher ratios of the surfactant,
316 were not possible to analyse using this method. However, assuming extrapolated effect, the
317 drug-polymer miscibility will be enhanced by approximately 1.5-2 folds when compared to
318 mixtures that did not contain any surfactants.

319

320 **Figure 4:** Flory-Huggins analysis of the thermodynamics of mixing using melting point
321 depression of physical mixtures of GF: HPMCAS and incorporating different ratios of the
322 surfactants. Some surfactant ratios were not possible to measure due to thermal degradation.

323

324 **Assessment of GF-HPMCAS miscibility using reduced onset of crystallization of** 325 **amorphous solid dispersions**

326 When heating the amorphous dispersion, the drug/ polymer molecules will gain sufficient
327 molecular mobility that will cause the solid dispersion to move to the rubbery state. Once the
328 dispersion is in the rubbery state, the molecules will move at significantly faster rate allowing
329 them to rearrange and recrystallize in the most stable crystalline structure. Additional heating
330 will lead to fusion event and liberation from the solid state. The onset of these events can be
331 used as a measure of drug miscibility in the solid dispersion. Here we use a combination of
332 analytical tools to assess the extent of drug-polymer miscibility which are melting point
333 depression and reduced onset of crystallization.

334

335 While the shifted onset of recrystallization temperature (T_c) can indicate altered kinetics for
336 recrystallization, the ratio between the T_c , T_g and T_m will be more precise method to predict
337 miscibility. The rationale for using this ratio is to establish a common scale for different
338 dispersions regardless of the measurement conditions. As such the minimum point on the scale
339 is the T_g and the maximum is T_m . This ratio can be described as the ratio of the difference
340 between onset of recrystallization temperature (T_c) and T_g to the difference between melting
341 point onset (T_m) and T_g [21].

342

343

$$R_c = \frac{T_c - T_g}{T_m - T_g}$$

344

345

346 Depending on the onset values of T_m , T_g and T_c , the ratio can be used to predict likelihood for
347 spontaneous recrystallization. Lower ratios implicate faster rate of recrystallization of
348 amorphous materials [22].

349

350 As can be seen in Figure 5, reduced recrystallization was different among prepared dispersions.
351 When compared with GF which was found to have recrystallization ratio of 0.32 [22], the
352 prepared dispersions showed higher values. For example, SDS containing solid dispersions
353 displayed R_c values between 0.48 to 0.58 with sharp reduction in R_c when the ratio of SDS was
354 increased to 5%. F127 solid dispersions showed the lowest recrystallization ratios with a range
355 between 0.44-0.46. Among the three surfactants, only DTAB solid dispersions showed positive
356 correlation between reduced recrystallization and surfactant ratio in the solid dispersion.
357 Overall, these results indicate that the extent of recrystallization follows the following trend
358 SDS>DTAB>F127 at low surfactant ratios and follows the following trend DTAB>SDS>F127 at
359 high surfactant ratios. Both DTAB and SDS solid dispersions showed higher ratios than the
360 spray dried amorphous solid dispersion prepared without surfactants. Hence, these results
361 suggest that incorporating DTAB and SDS (within tested range) may increase physical stability
362 of the amorphous form. It is worth mentioning that the onset values were used to perform the
363 analysis; all samples did not exhibit thermal degradation within the onset melting temperature.

364

365 **Figure 5:** Reduced recrystallization of spray dried amorphous solid dispersions of GF:
366 HPMCAS (50%:50%) containing varied ratios of the surfactants. The x symbol represents the
367 value for spray dried amorphous solid dispersion without surfactants.

368

369 Pearson correlation coefficient (r) values for linear trends in Figure 5 were calculated and
370 showed that DTAB had r value of 0.84 while SDS and F127 dispersions showed r values of -
371 0.96 and -0.98, respectively. This analysis indicates strong linear relationship between the
372 surfactant ratio and the reduced recrystallization values. The positive r indicates that increasing
373 DTAB ratio in the dispersion increased R_c while the opposite trend was correct for SDS and
374 F127.

375

376

377 **Aqueous saturated solubility measurements**

378 The saturation solubility of spray dried amorphous solid dispersions and corresponding physical
379 mixtures was measured in phosphate buffer (pH 6.8). As can be seen in Figure 6, the solid
380 dispersions of GF and HPMCAS with SDS exhibited higher GF aqueous solubilities than the
381 corresponding physical mixtures with solubilities in the range of 101-121 $\mu\text{g}/\text{mL}$. This value was
382 higher than the solid dispersions of GF and HPMCAS prepared in the absence of surfactant that
383 showed solubility of 88 $\mu\text{g}/\text{mL}$. On the other hand, solid dispersions of GF and HPMCAS with
384 F127 showed solubility results comparable to or slightly higher than the corresponding physical
385 mixtures. Increasing the ratio of F127 from 1% to 5% led to lower solubility values of 115 and
386 84 $\mu\text{g}/\text{mL}$, respectively. Solid dispersions of GF and HPMCAS with DTAB showed even lower
387 solubility values than SDS and F127 containing solid dispersions. Increasing the ratio of DTAB
388 from 1% to 5% has led to lower solubility values of 74 and 42 $\mu\text{g}/\text{mL}$, respectively.

389

390 **Figure 6:** Saturated aqueous solubility measurements of spray dried amorphous solid
391 dispersions (SD) of GF: HPMCAS (50%: 50%) containing varied ratios of surfactants and
392 compared with corresponding physical mixtures (PM).

393

394 Analysis of surfactants micellar solutions showed that SDS achieved significant enhancement in
395 GF solubility (Figure 7). The micellar solutions were prepared using mass ratio in distilled water
396 via adding excess amount of GF to determine saturation solubility. Saturation solubility
397 exceeded 6mg/mL for SDS while for DTAB was around 1.6mg/L and 0.1 mg/L for F127. It is
398 interesting to observe that these trends did not correlate with GF solubility when it was
399 dissolved as a solid dispersion. It is evident from Figure 6 that the cationic DTAB showed
400 reduced solubility compared with SDS and F127 which could be attributed to forming ionic
401 interactions with the acidic HPMCAS. It is also interesting to see that F127 solid dispersions
402 displayed similar solubility to the micellar solutions despite that the F127 content is significantly
403 less in the solid dispersions. When comparing the critical micellar concentrations (CMC), the
404 following trends can be seen DTAB>SDS>F127 (DTAB 15 mM, SDS 8.25 mM, F127 0.357 mM)
405 [15-17]. Hence, it is possible that the low CMC of F127 meant that micelles could be present
406 when the solid dispersions were dissolved.

407

408 **Figure 7:** Saturated solubility of GF in micellar solutions of different w/v% ratios of SDS, DTAB,
409 F127.

410

411

412 **Correlation between predicted and experimental solubility**

413 Originally used to calculate solubility ratio of glucose glass to α -glucose crystals, equation 4 has
414 been widely used to predict solubility ratio between the amorphous/crystalline forms ($\frac{\sigma_a}{\sigma_c}$) [23],

415

$$\Delta G_{c \rightarrow a} = -RT \ln \frac{\sigma_a}{\sigma_c} \quad (1)$$

416
417 (4)

418 Where R is the gas constant and $\Delta G_{c \rightarrow a}$ is the free energy changes associated with the
419 conversion of the amorphous to the crystalline form.

420

421 Prediction of the solubility ratio is based on the assumption that the additional free energy of the
422 amorphous form is proportional to the increase in kinetic energy leading to enhanced solubility.
423 A possible theoretical approach to predict the difference in solubility of the amorphous as
424 compared to the crystalline form is via the use of Hoffman's equation to calculate the total free
425 energy change associated from the crystalline to the amorphous form ($\Delta G_{c \rightarrow a}$) [24],

426

$$\Delta G_{c \rightarrow a} = \frac{\Delta H \cdot T (T_m - T)}{T_m^2}$$

427
428 (5)

429

430 By which ΔH is the enthalpy of fusion and T being the temperature of interest.

431

432 As can be seen in Figure 8, the solubility ratio of GF at 298.15 K is approximately 65 with
433 configurational free energy of 10.4 kJ/mol. The rapid recrystallization of GF makes it difficult to
434 experimentally determine the amorphous form solubility hence this method represents a good
435 approximation of solubility enhancement of fully amorphous GF. As can be seen, the
436 configurational free energy decreased with increasing the temperature indicating that glass GF
437 will exhibit maximum solubility around 298.15 K. This value does not take in consideration any
438 kinetic contributions to increasing the solubility but is purely based on free energy excess of the
439 amorphous form.

440

441 **Figure 8:** Solubility ratio (amorphous/crystalline) of GF versus configurational energy.

442

443 Experimental solubility measurements of amorphous solid dispersions were used to calculate
444 the solubility ratios relative to the solubility of crystalline GF (Figure 9). As can be seen, the
445 solubility ratio of the amorphous solid dispersions (without surfactants) was found to be 8.8.
446 This is significantly lower than the expected value for amorphous GF which may indicate
447 possible recrystallization during dissolution. We have shown before that amorphous solid
448 dispersions exhibited time dependent solubility by which a peak concentration was observed
449 after 1 hour [25]. The assumption of amorphous form higher solubility should therefore be
450 evaluated within the same time frame. Maintaining GF as amorphous for 72 hours is not
451 possible as it tends to crystallize within hours when stored at dry conditions. Practically,
452 solubility of amorphous GF cannot be determined accurately because recrystallization happens
453 so fast which makes determination of this value largely hypothetical. The results show positive
454 impact when SDS was incorporated with a solubility ratio range between 10-12. The lower
455 solubility of DTAB solid dispersion can be clearly seen with solubility ratios reaching 4 indicating
456 that the drug solubility was halved when compared with the dispersions that did not contain any
457 surfactants. Opposite to SDS dispersions, F127 initially enhanced the solubility ratio but was
458 decreased when the F127 ratio was increased to 5%.

459

460 **Figure 9:** Experimental solubility ratios of GF from amorphous solid dispersions compared with
461 the experimentally determined solubility of crystalline GF.

462

463 As can be seen in Figure 10, reduced recrystallization was lowest for F127 containing solid
464 dispersions. When the ratio of the F127 was increased from 1% to 5%, reduced
465 recrystallization decreased which was also associated with lower solubility. This trend was
466 reversed in the case of DTAB solid dispersions which was associated with reduced solubility
467 values. SDS solid dispersion showed slightly variable solubility ratio which was affected to less
468 extent by R_c . These results suggest that the surfactants may affect nucleation and possibly
469 crystal growth upon exposure to aqueous media. Furthermore, solubility differences between
470 physical mixtures and spray dried solid dispersions reflect key role for the amorphous form and
471 the molecular interactions with the polymer.

472

473 **Figure 10:** Reduced crystallization of spray dried amorphous solid dispersions against
474 experimental solubility ratio.

475

476 **Spectroscopic analysis of solid dispersions**

477 FTIR was carried out to identify if there was a possible hydrogen bonding between the GF and
478 HPMCAS, and to assess whether the presence of surfactants affects this interaction. The
479 absorbances between 1750 and 1550 cm^{-1} correspond to the C=O stretch of the benzofuran ring
480 and cyclohexene, and C=C stretch of the cyclic rings of the structure shown in Figure 11. GF has
481 two peaks which correspond to the two carbonyl groups, so there are two distinctive peaks; the
482 first at 1712 cm^{-1} which corresponds to stretching of the C=O in the benzofuran ring and the
483 second peak at 1662 cm^{-1} which corresponds to C=O of cyclohexene. It was shown before that
484 the presence of HPMCAS caused a broadening of carbonyl peak at 1662 cm^{-1} which is an
485 indication of hydrogen bonding been present which results in a shift of peak to the right to a lower
486 frequency [7]. Presence of amorphous GF formation can be confirmed by the disappearance of
487 peaks at 1220, 1350 and 1580 cm^{-1} . Overall, the presence of the surfactants did not affect the
488 peaks positions, nor the broadening seen in the GF/ HPMCAS solid dispersions indicating no
489 alteration of polarity around aforementioned groups.

490

491 **Figure 11:** FTIR spectra showing (a) GF, HPMCAS, GF: HPMCAS solid dispersion (50%:50%)
492 (SD) and corresponding physical mixture (PM). The arrows indicate peaks that disappeared when
493 amorphous GF was formed and (b) SD of GF: HPMCAS (50%:50%) with 5% surfactants showing
494 no difference in peaks positions compared with (GF: HPMCAS) SD.

495

496

497

498 **Particle size and morphology analysis of solid dispersions**

499 Particle size analysis showed that the GF: HPMCAS physical mixtures prepared with different
500 surfactants ratios had a particle size range between 10-20 μm (Figure 12). It is interesting to
501 observe that surfactants caused larger particle size distribution when compared with the
502 GF:HPMCAS mixtures. Such behaviour may suggest bridging the polymer chain through the
503 surfactant forming larger aggregates. The trend seemed stronger in the following order
504 SDS>DTAB>F127 reflecting differences in the intermolecular interactions promoting aggregate
505 formation. Opposite to this trend is the particle size analysis of spray dried solid dispersions which
506 showed that F127 particles were larger than SDS and DTAB dispersions.

507

508 **Figure 12:** Particle size analysis of GF: HPMCAS physical mixtures prepared with different
509 surfactants ratios. Also shown is the particle size analysis of amorphous solid dispersions of GF:
510 HPMCAS (50%:50%) prepared with different surfactants ratios.

511

512 To understand whether the trends observed above were due to the exposure to aqueous media
513 which could have induced aggregations, scanning electron microscopy images were used to analyse
514 morphology and particle size in the solid state (Figure 13). As can be seen, the particles were
515 spherical with particle size distribution smaller for F127 solid dispersions suggesting that the
516 particle size growth was promoted by the aqueous media used when measuring the particles size.

517

518 **Figure 13:** Scanning electron microscopy showing spray dried amorphous solid dispersions of
519 GF: HPMCAS (50%:50%) with (a) 2.5% DTAB, (b) 2.5% F127, (c) 2.5% SDS and (d) no
520 surfactants.

521

522

523 **Discussion**

524 The results presented in this research showed that surfactants can enhance the solid state
525 miscibility of the model drug GF with HPMCAS. The enhanced solid state miscibility can be
526 attributed to lowering the heat of mixing which can interfere with the extent of mixing. The extent
527 of this lowering was found to be highest when DTAB was used. After spray drying, the drug-
528 polymer interactions are expected to mirror the interactions observed in the melted physical
529 mixtures. The main difference would be the impact of the solvent on whether it can hinder or limit
530 intermolecular interactions. As was seen, it was possible to see a correlation between the
531 reduced crystallization parameter which represents the difference in glass transition,
532 crystallization and melting temperatures. It is expected that enhanced solid state miscibility will
533 be translated as enhanced saturated solubility. This expectation is based on the fact that
534 HPMCAS is a hydrophilic polymer and enhanced miscibility is a result of increased intermolecular
535 contacts with the drug and therefore improve the saturated solubility. When surfactants were
536 incorporated into the solid dispersions, the solubility decreased with a trend that suggests lack of
537 micellar solubilization. This conclusion was based on comparison with micellar solubility of GF
538 suggesting that the surfactants chains were molecularly associated with HPMCAS.

539

540 The lowest solubility was found in DTAB solid dispersions which could potentially be attributed to
541 electrostatic interactions with HPMCAS. There were no signs of disruption of the intermolecular
542 hydrogen bonding of GF with HPMCAS as evident from FTIR analysis hence all events observed
543 above can be attributed to exposure to the aqueous media. Based on particle size analysis, a
544 possible explanation would be that the growth of the particle size can be due to gelation

545 happening during the dissolution process which was particularly promoted by the polymeric
546 nature of F127. The intermolecular interactions were clearly very different from the physical
547 mixtures reflected in different particles size distribution. Overall, these data showed that the role
548 of surfactant is a complex role and can significantly be altered upon exposure to the dissolution
549 media.

550

551 Miscibility in the solid state can certainly be enhanced but that depends on the nature of
552 intermolecular interactions. Nevertheless, solid state miscibility may not be a prerequisite for a
553 better dissolution as the presence of water can promote particles aggregation. The type of
554 surfactant is critical for enhanced miscibility of the drug with the polymer; hence screening can be
555 used to select the optimum surfactant ratio while preventing possible recrystallization upon
556 dissolution. While there is no evidence of forming localised regions of amorphous drug within
557 surfactant aggregates, lowered saturated solubility cannot solely be attributed to recrystallization
558 of the amorphous drug. Hence, it is possible that the drug is localized within micro amorphous
559 domains prior to dissolution resembling micellar structures. These structures remain hypothetical
560 and will be the focus of future research.

561

562 **Conclusions**

563 The impact of incorporating surfactants on thermodynamic parameters was assessed.
564 Overall trend showed that DTAB containing solid dispersions had highest miscibility when
565 compared with other dispersions. However, when comparing saturated solubility, the
566 impact on solubility was reversed. The findings of this work highlight, for the first-time,
567 potential correlation between phase transition temperatures and drug polymer miscibility
568 which can be used to design amorphous dispersions with enhanced properties. While
569 there was a positive impact in terms of enhancing drug-polymer miscibility, the impact on
570 saturation solubility requires further investigation.

571

572

573 **Conflicts of interest**

574 There are no conflicts to declare.

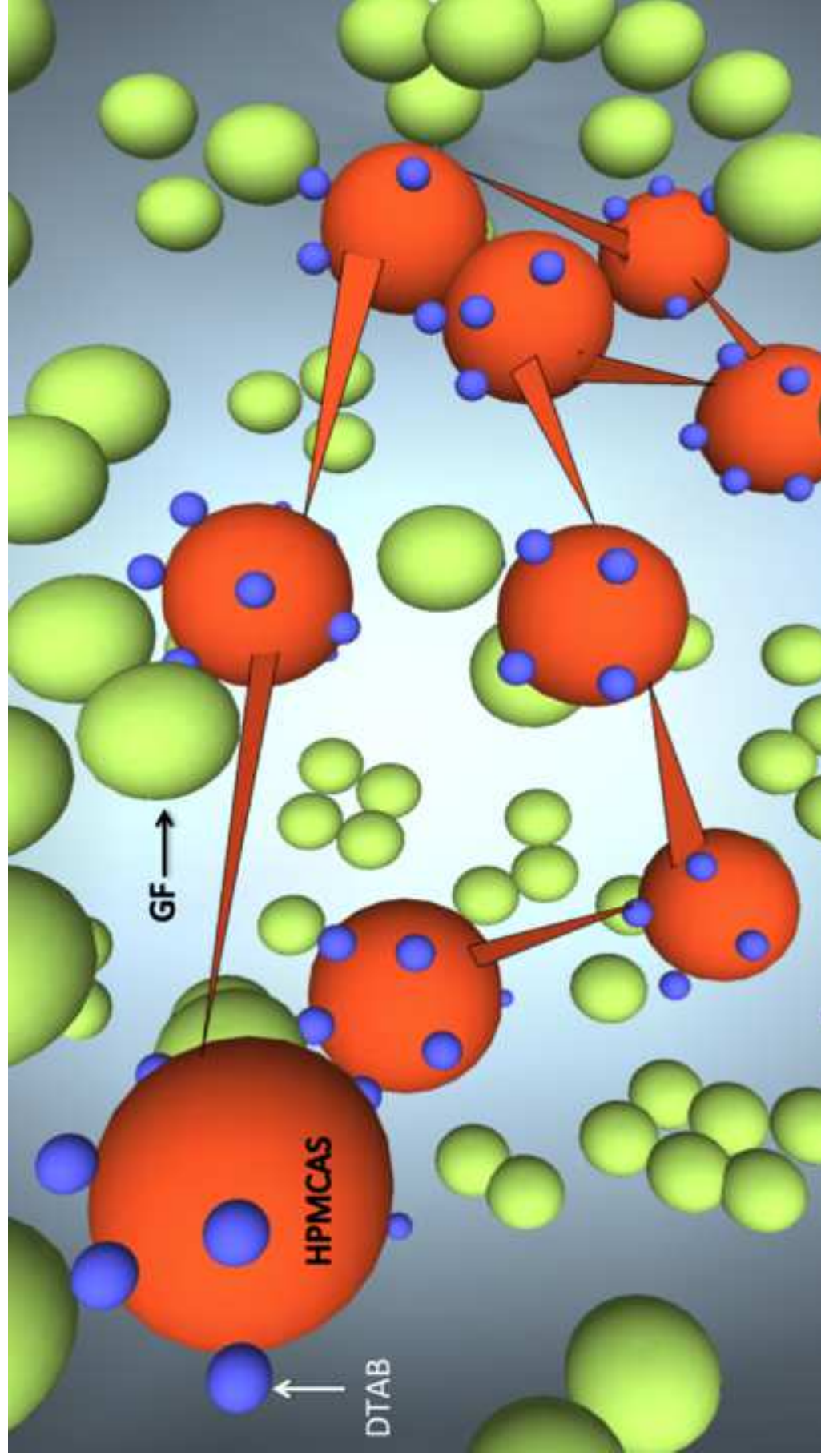
575

576 **Acknowledgements**

577 The authors would like to thank the Chemical Analysis Facility at the University of
578 Reading for providing essential access to instruments used in this study.

580 **References**

- 581 [1] H.H. Tong, Z. Du, G.N. Wang, H.M. Chan, Q. Chang, L.C. Lai, A.H. Chow, Y. Zheng, Spray freeze drying with polyvinylpyrrolidone and sodium
582 caprate for improved dissolution and oral bioavailability of oleanolic acid, a BCS Class IV compound, *International journal of pharmaceuticals*,
583 404 (2011) 148-158.
- 584 [2] J.A. Baird, L.S. Taylor, Evaluation of amorphous solid dispersion properties using thermal analysis techniques, *Adv Drug Deliv Rev*, (2011).
- 585 [3] B. Li, S. Konecke, L.A. Wegiel, L.S. Taylor, K.J. Edgar, Both solubility and chemical stability of curcumin are enhanced by solid dispersion in
586 cellulose derivative matrices, *Carbohydrate polymers*, 98 (2013) 1108-1116.
- 587 [4] P. Srinarong, H. de Waard, H.W. Frijlink, W. Hinrichs, Improved dissolution behavior of lipophilic drugs by solid dispersions: the production
588 process as starting point for formulation considerations, *Expert Opin Drug Deliv*, 8 (2011) 1121-1140.
- 589 [5] D. Horter, J.B. Dressman, Influence of physicochemical properties on dissolution of drugs in the gastrointestinal tract, *Adv Drug Deliv Rev*,
590 46 (2001) 75-87.
- 591 [6] R. Laitinen, E. Suihko, M. Bjorkqvist, J. Riikonen, V.P. Lehto, K. Jarvinen, J. Ketolainen, Perphenazine solid dispersions for orally fast-
592 disintegrating tablets: physical stability and formulation, *Drug Dev Ind Pharm*, 36 (2010) 601-613.
- 593 [7] H. Al-Obaidi, G. Buckton, Evaluation of griseofulvin binary and ternary solid dispersions with HPMCAS, *AAPS PharmSciTech*, 10 (2009)
594 1172-1177.
- 595 [8] J.A. Baird, B. Van Eerdenbrugh, L.S. Taylor, A classification system to assess the crystallization tendency of organic molecules from
596 undercooled melts, *Journal of pharmaceutical sciences*, 99 (2010) 3787-3806.
- 597 [9] H. Al-Obaidi, M.J. Lawrence, S. Shah, H. Moghul, N. Al-Saden, F. Bari, Effect of drug-polymer interactions on the aqueous solubility of
598 milled solid dispersions, *International journal of pharmaceuticals*, 446 (2013) 100-105.
- 599 [10] M. Aldén, M. Lydén, J. Tegenfeldt, Effect of counterions on the interactions in solid dispersions between polyethylene glycol, griseofulvin
600 and alkali dodecyl sulphates, *Int. J. Pharm.*, 110 (1994) 267-276.
- 601 [11] M. Wulff, M. Aldén, D.Q.M. Craig, An investigation into the critical surfactant concentration for solid solubility of hydrophobic drug in
602 different polyethylene glycols, *Int. J. Pharm.*, 142 (1996) 189-198.
- 603 [12] S. Sheokand, J. Sharma, A.K. Bansal, Effect of surfactants on the molecular mobility and crystallization kinetics of hesperetin,
604 *CrystEngComm*, 21 (2019) 3788-3797.
- 605 [13] T.M. Deshpande, H. Shi, J. Pietryka, S.W. Hoag, A. Medek, Investigation of Polymer/Surfactant Interactions and Their Impact on
606 Itraconazole Solubility and Precipitation Kinetics for Developing Spray-Dried Amorphous Solid Dispersions, *Mol Pharmaceut*, 15 (2018) 962-
607 974.
- 608 [14] H. Al-Obaidi, M.J. Lawrence, G. Buckton, Atypical effects of incorporated surfactants on stability and dissolution properties of amorphous
609 polymeric dispersions, *The Journal of pharmacy and pharmacology*, 68 (2016) 1373-1383.
- 610 [15] V. Peyre, S. Bouguerra, F. Testard, Micellization of dodecyltrimethylammonium bromide in water-dimethylsulfoxide mixtures: a multi-
611 length scale approach in a model system, *Journal of colloid and interface science*, 389 (2013) 164-174.
- 612 [16] Y. Moroi, K. Motomura, R. Matuura, The critical micelle concentration of sodium dodecyl sulfate-bivalent metal dodecyl sulfate mixtures
613 in aqueous solutions, *J Colloid Interface Sci*, 46 (1974) 111-117.
- 614 [17] L.M.U. Dutra, M.E.N.P. Ribeiro, I.M. Cavalcante, D.H.A.d. Brito, L.d.M. Semião, R.F.d. Silva, P.B.A. Fechine, S.G. Yeates, N.M.P.S. Ricardo,
615 Binary mixture micellar systems of F127 and P123 for griseofulvin solubilisation, *Polímeros*, 25 (2015) 433-439.
- 616 [18] H. Al-Obaidi, P. Ke, S. Brocchini, G. Buckton, Characterization and stability of ternary solid dispersions with PVP and PHPMA, *International*
617 *journal of pharmaceuticals*, 419 (2011) 20-27.
- 618 [19] P.J. Marsac, H. Konno, A.C. Rumondor, L.S. Taylor, Recrystallization of nifedipine and felodipine from amorphous molecular level solid
619 dispersions containing poly(vinylpyrrolidone) and sorbed water, *Pharmaceutical research*, 25 (2008) 647-656.
- 620 [20] J. Djuris, I. Nikolakakis, S. Ibric, Z. Djuric, K. Kachrimanis, Preparation of carbamazepine-Soluplus solid dispersions by hot-melt extrusion,
621 and prediction of drug-polymer miscibility by thermodynamic model fitting, *European journal of pharmaceuticals and biopharmaceutics* :
622 official journal of Arbeitsgemeinschaft fur Pharmazeutische Verfahrenstechnik e.V, 84 (2013) 228-237.
- 623 [21] D. Zhou, G.G. Zhang, D. Law, D.J. Grant, E.A. Schmitt, Physical stability of amorphous pharmaceuticals: Importance of configurational
624 thermodynamic quantities and molecular mobility, *Journal of pharmaceutical sciences*, 91 (2002) 1863-1872.
- 625 [22] P. Gupta, G. Chawla, A.K. Bansal, Physical Stability and Solubility Advantage from Amorphous Celecoxib: The Role of Thermodynamic
626 Quantities and Molecular Mobility, *Mol Pharmaceut*, 1 (2004) 406-413.
- 627 [23] G.S. Parks, L.J. Snyder, F.R. Cattoir, Studies on glass. XI. Some thermodynamic relations of glassy and alpha-crystalline glucose, *J Chem*
628 *Phys*, 2 (1934) 595-598.
- 629 [24] J.D. Hoffman, Thermodynamic driving force in nucleation and growth processes, *J Chem Phys*, 29 (1958) 1192-1193.
- 630 [25] H. Al-Obaidi, M.J. Lawrence, N. Al-Saden, P. Ke, Investigation of griseofulvin and hydroxypropylmethyl cellulose acetate succinate
631 miscibility in ball milled solid dispersions, *International journal of pharmaceuticals*, 443 (2013) 95-102.



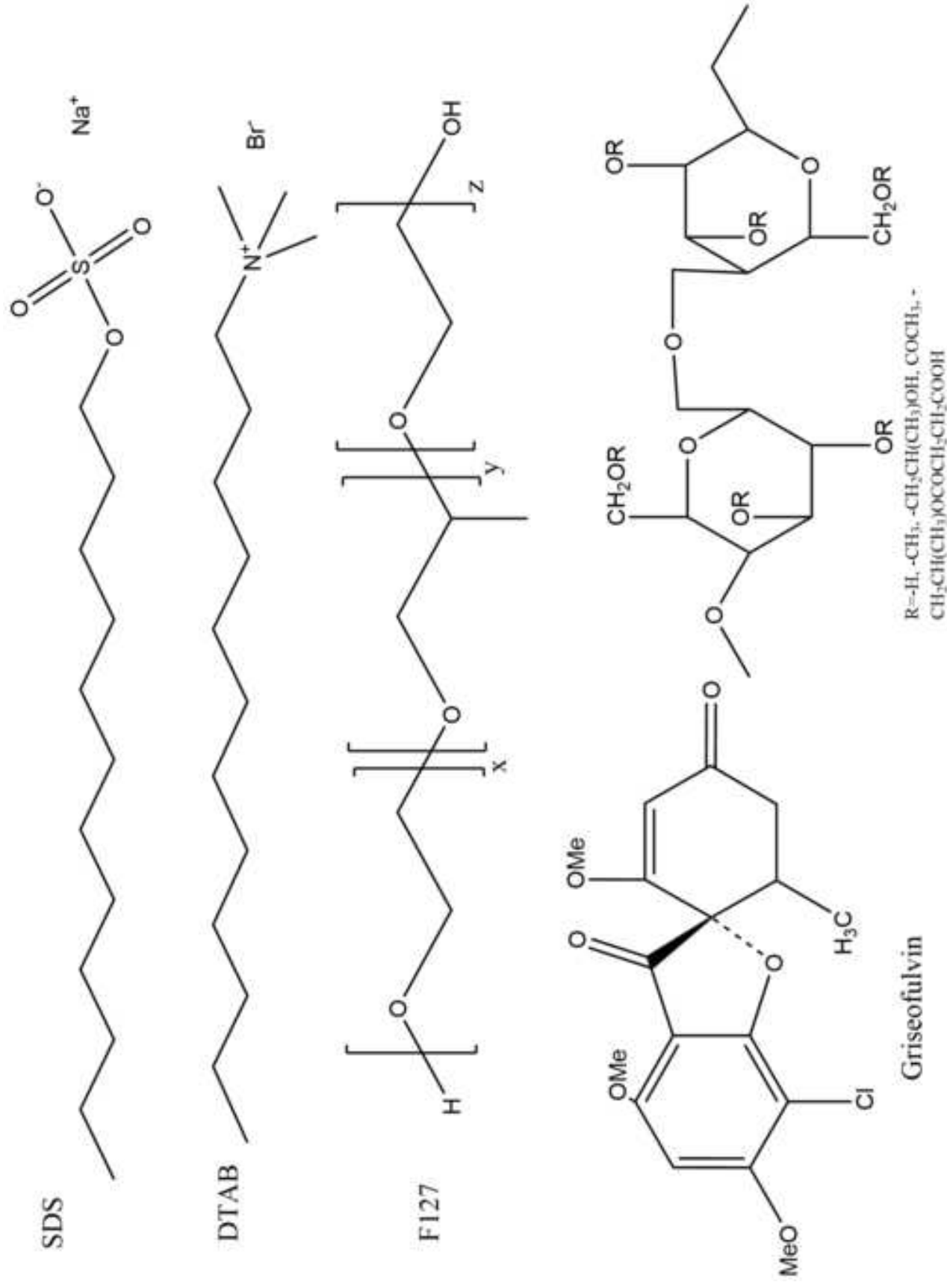


Figure 2a

[Click here to access/download;Figure;Figure 2_a.jpg](#)

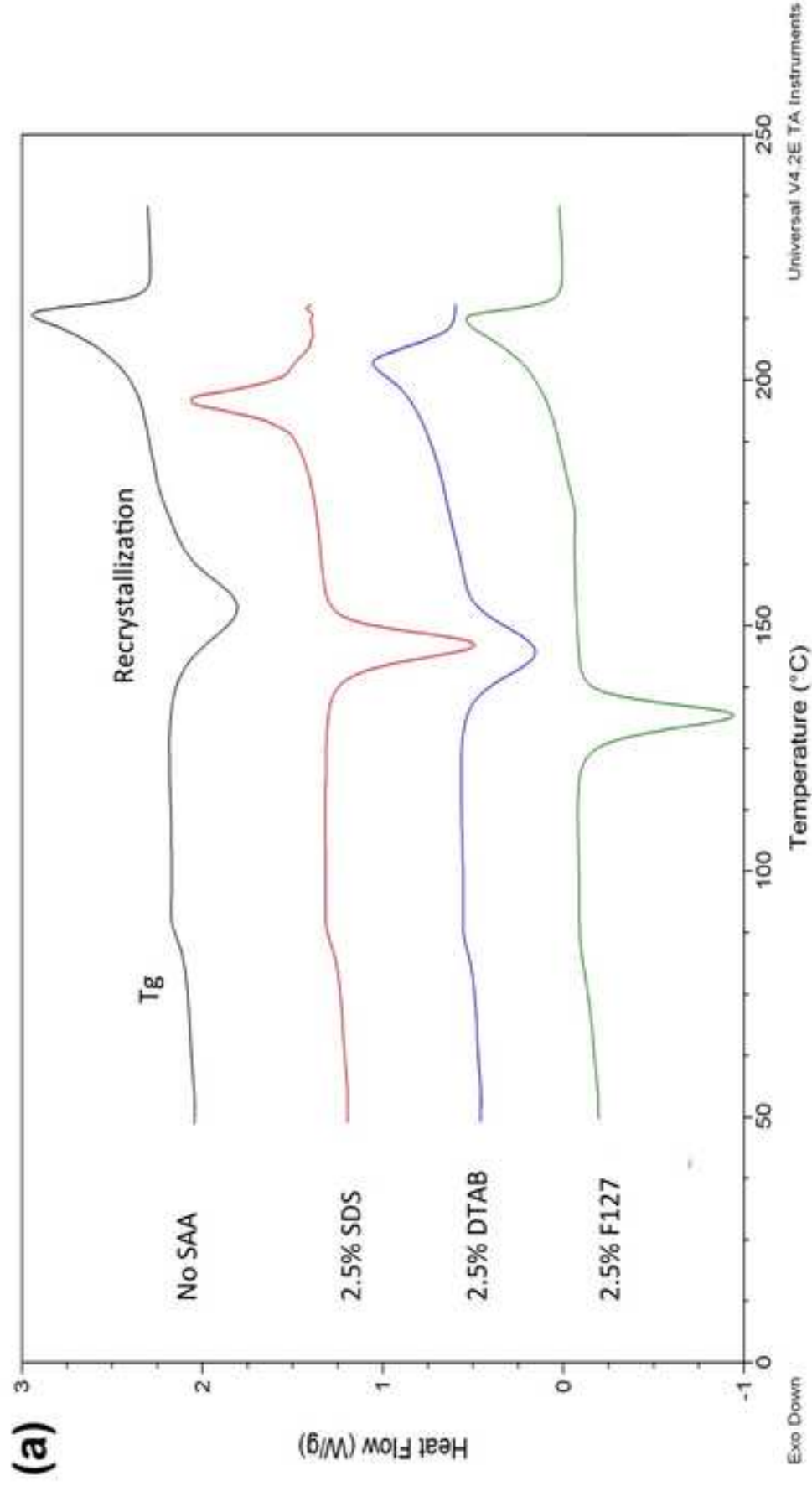


Figure 2b

[Click here to access/download;Figure;Figure 2_b.jpg](#)

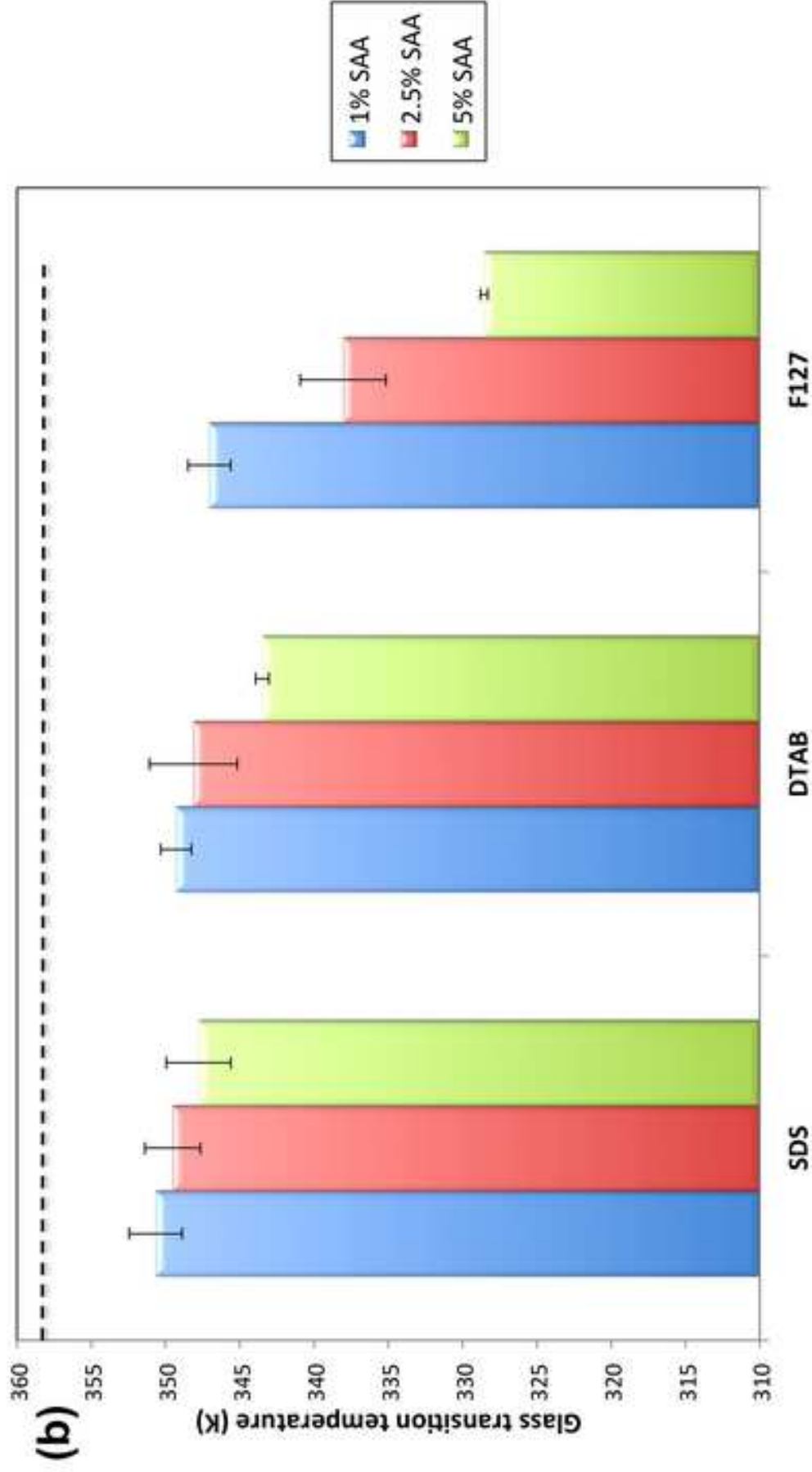
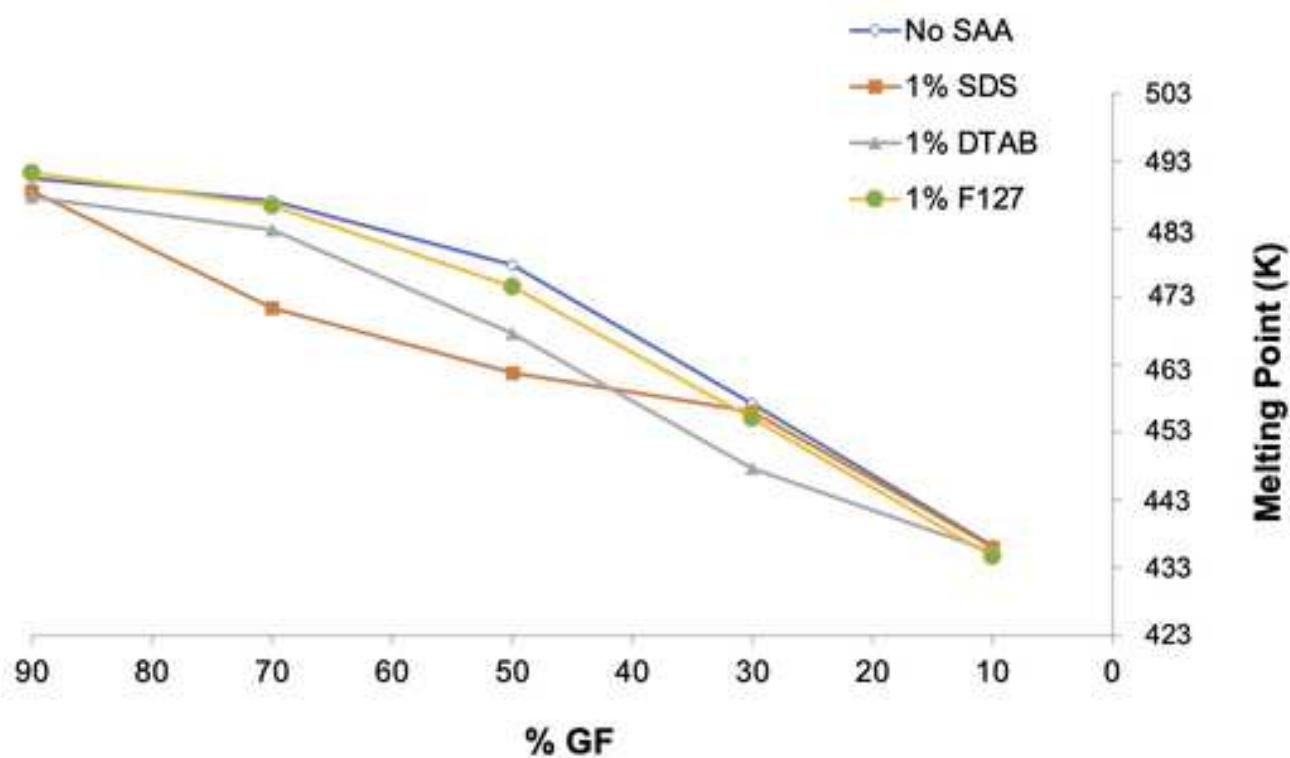


Figure 3

[Click here to access/download;Figure;Figure 3_.jpg](#)

(a)



(b)

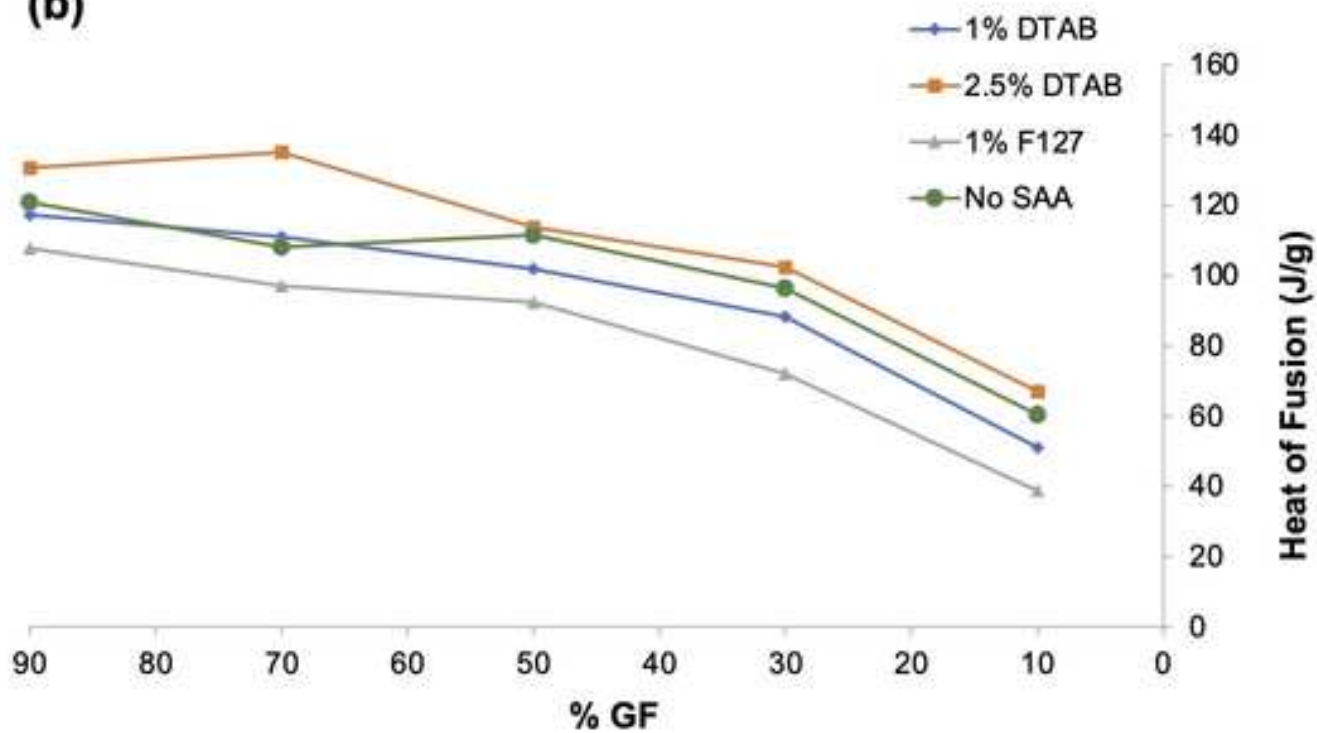


Figure 4

[Click here to access/download;Figure;Figure 4_.jpg](#)

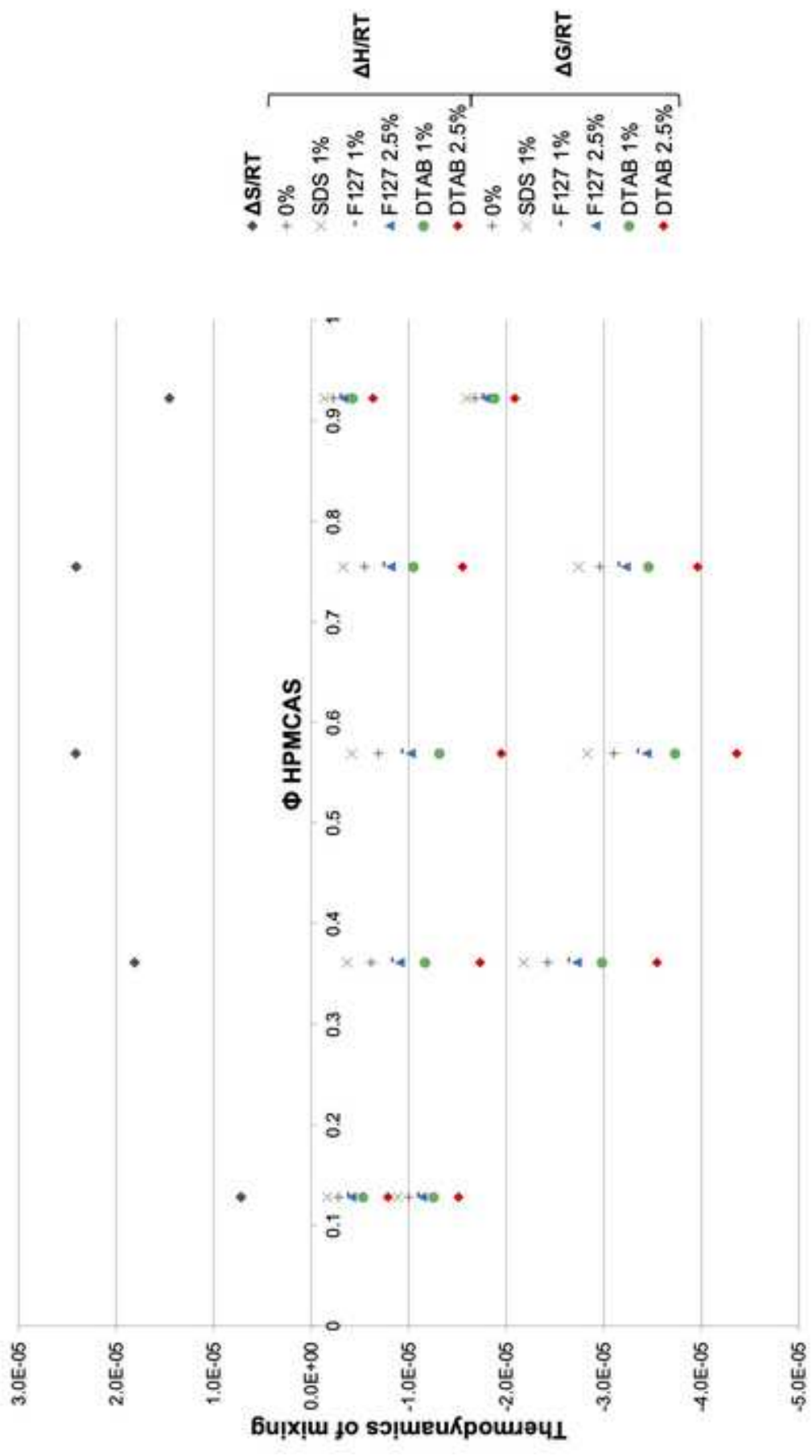


Figure 5

[Click here to access/download;Figure;Figure 5_.jpg](#)

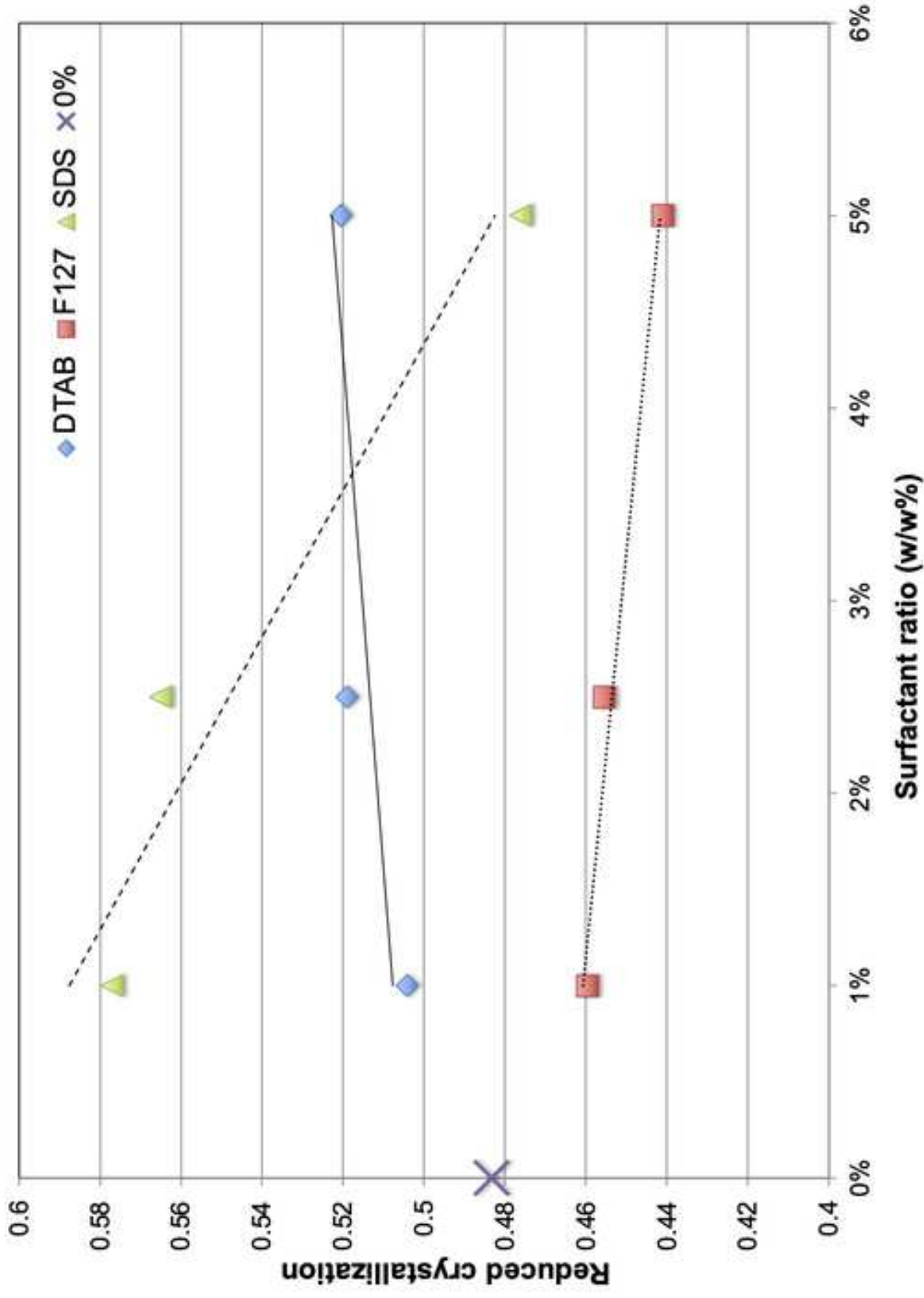


Figure 6

[Click here to access/download;Figure;Figure 6_.jpg](#)

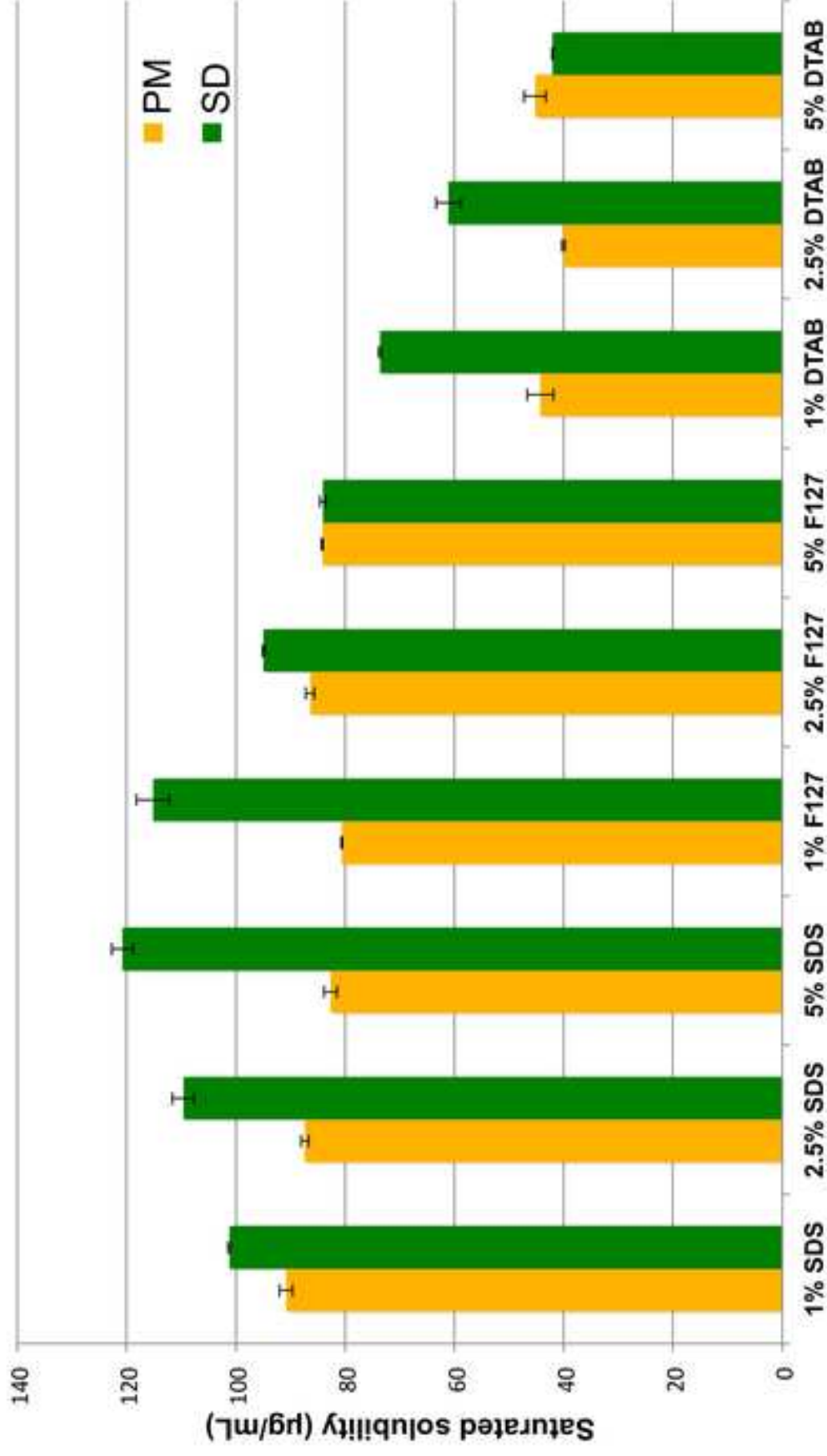


Figure 7

[Click here to access/download;Figure;Figure 7_.jpg](#)

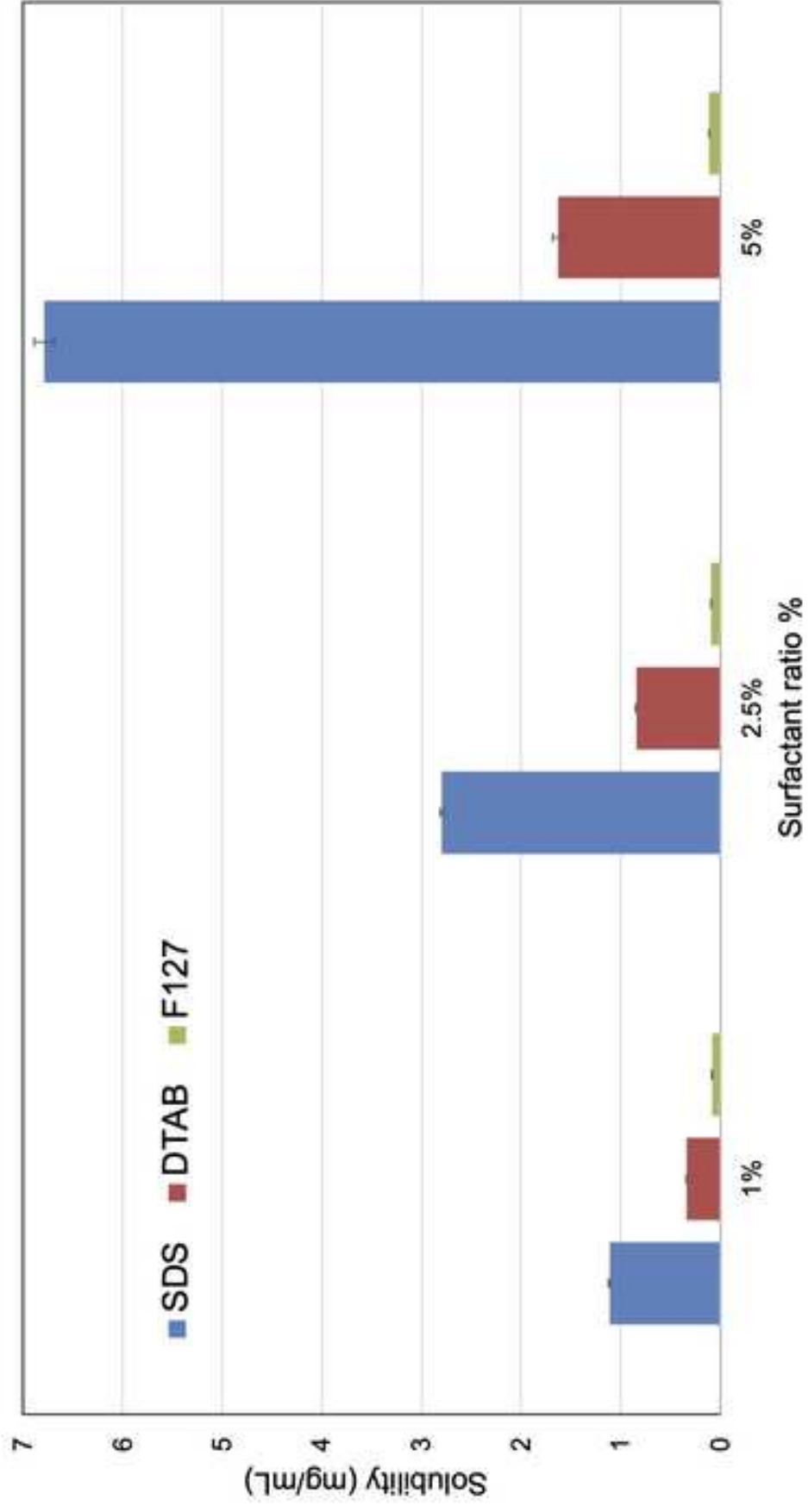


Figure 8

[Click here to access/download;Figure;Figure 8_.jpg](#)

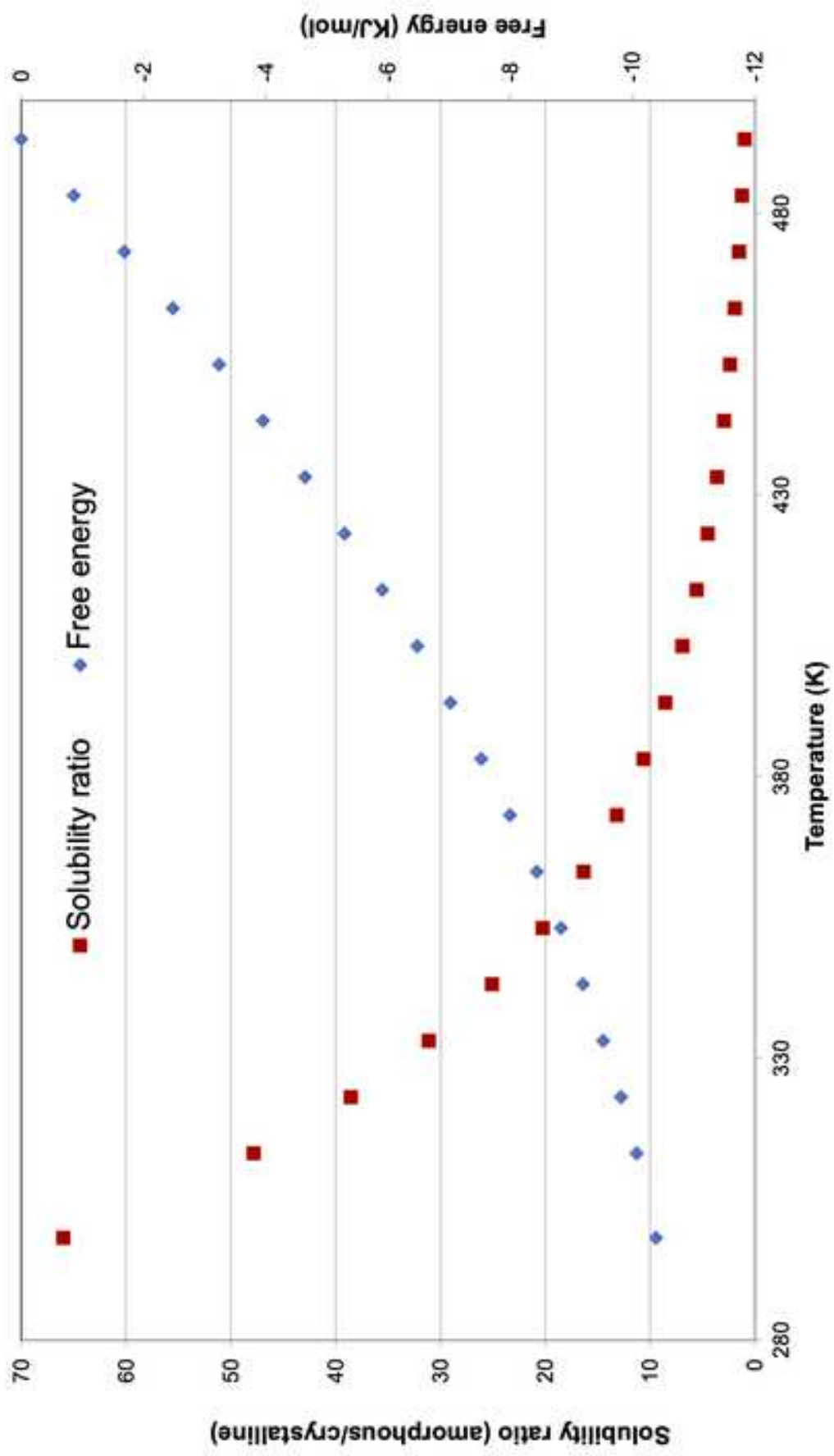


Figure 9

[Click here to access/download;Figure;Figure 9_.jpg](#)

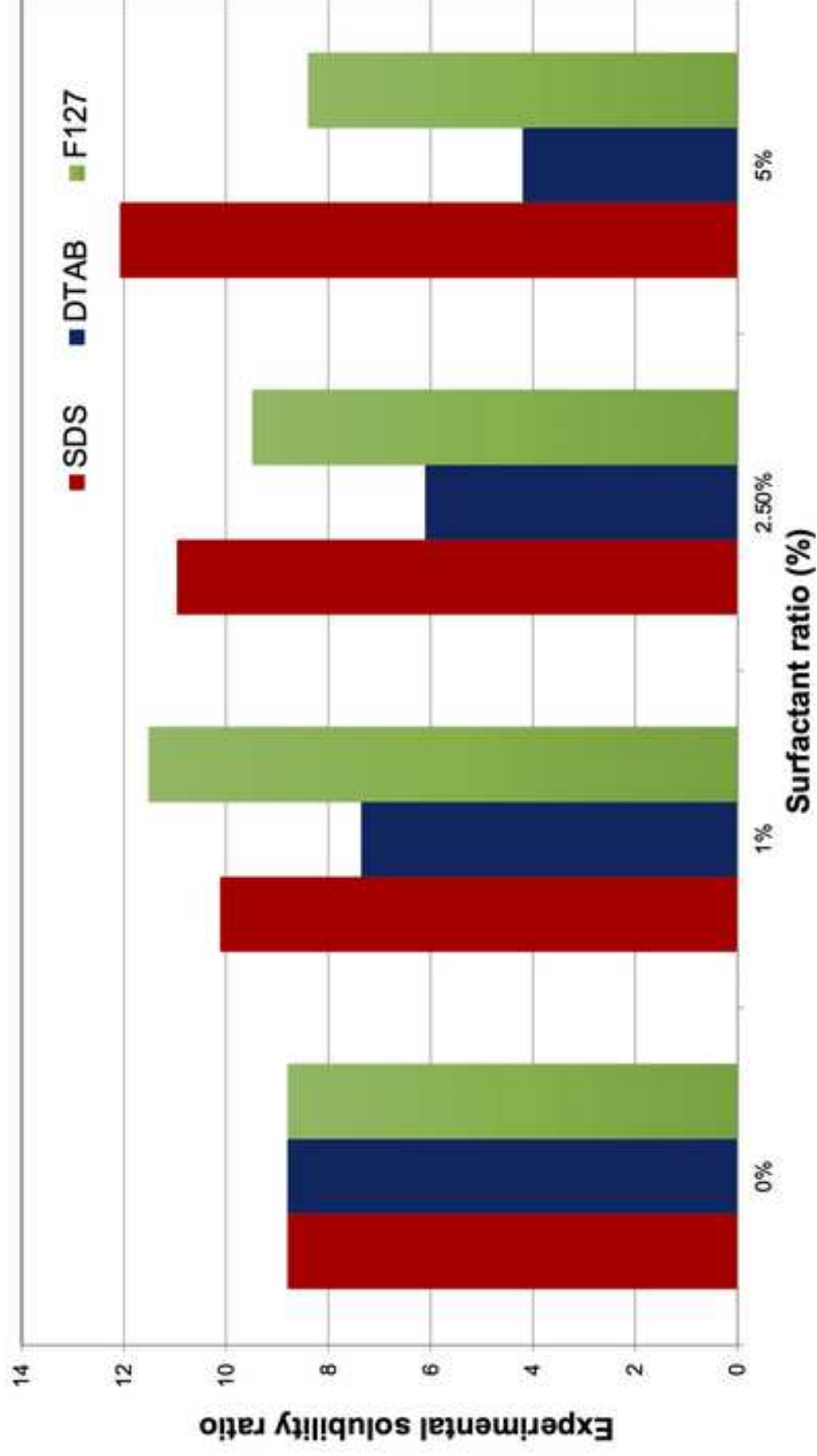


Figure 10

[Click here to access/download;Figure;Figure 10_.jpg](#)

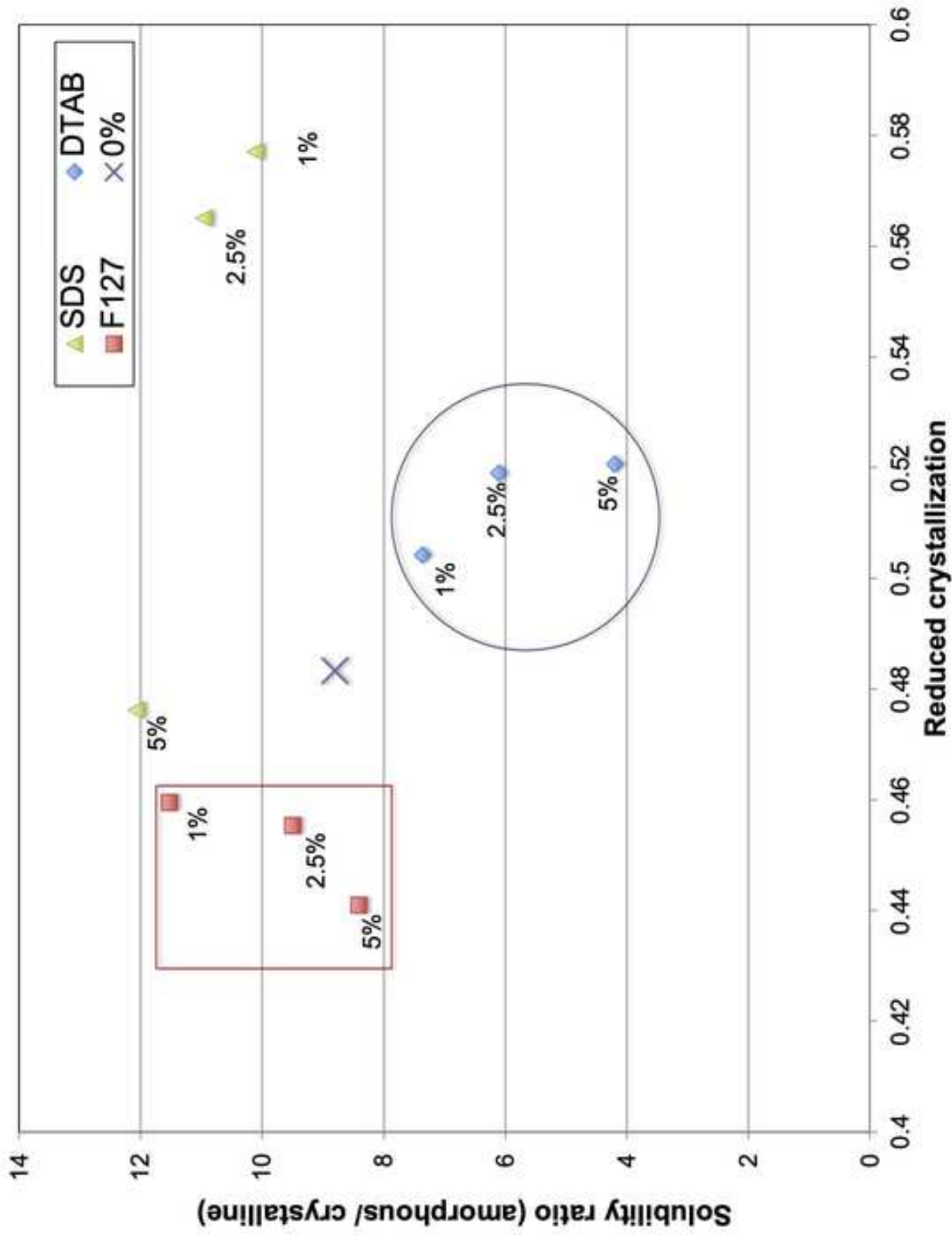
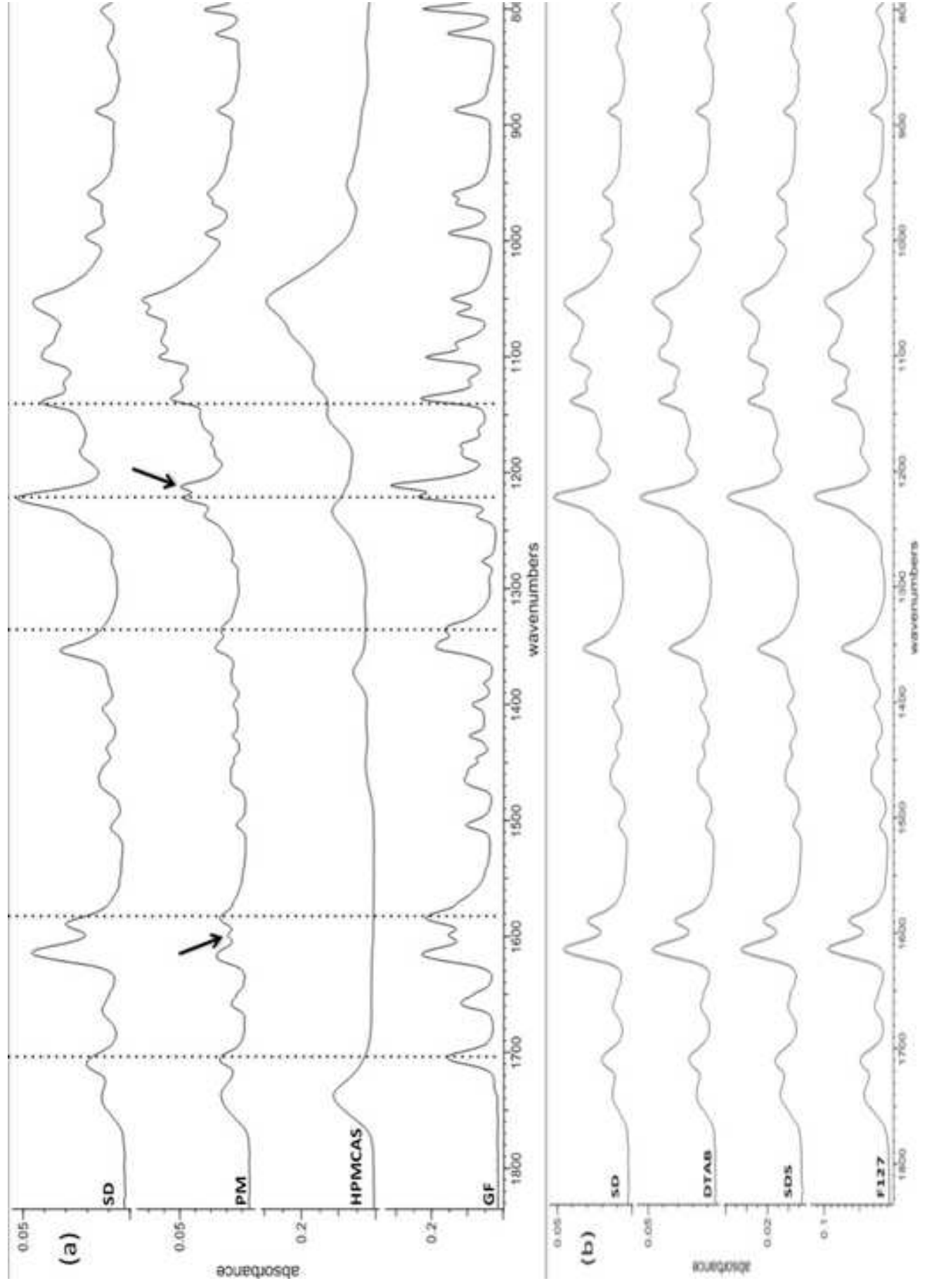
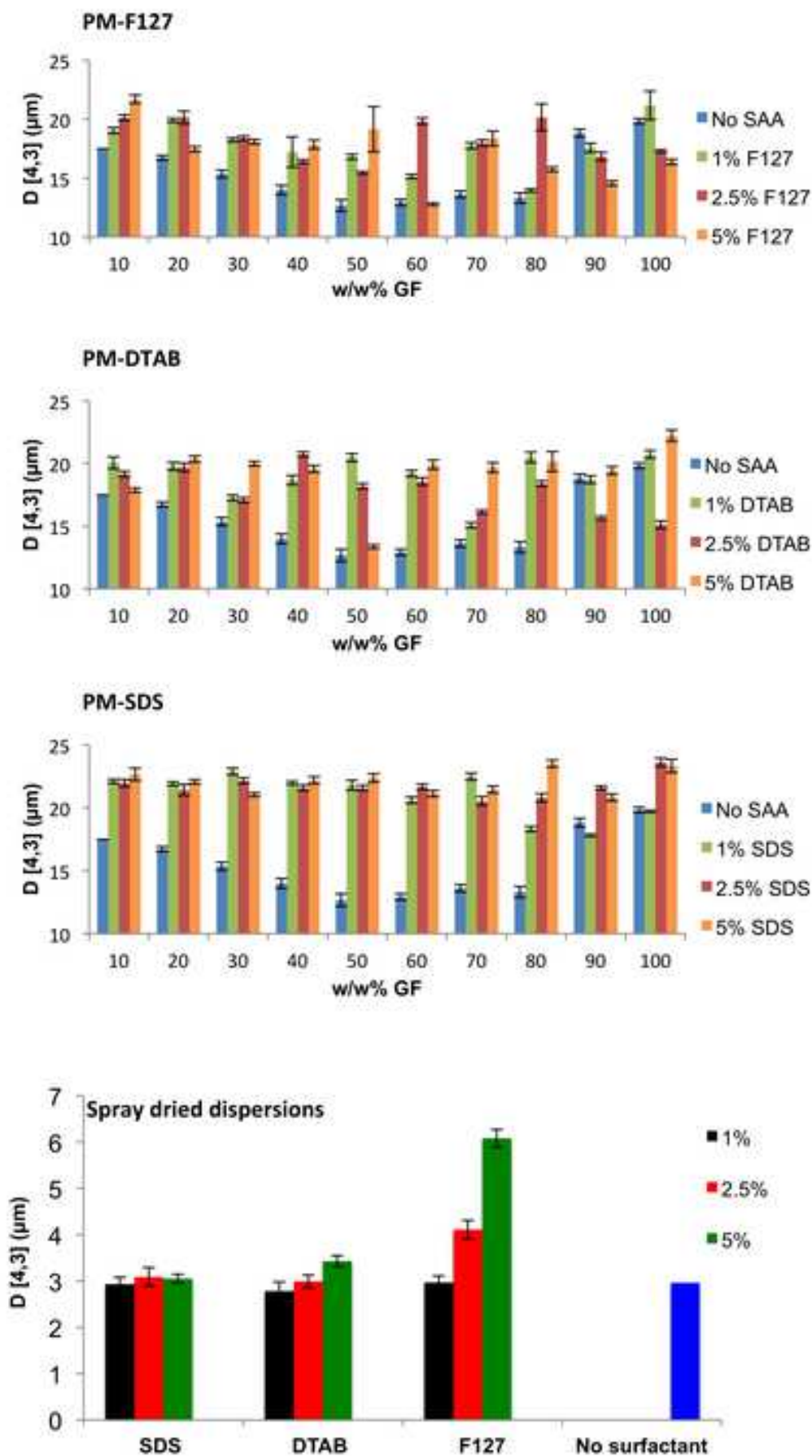


Figure 11

[Click here to access/download;Figure;Figure 11_.jpg](#)





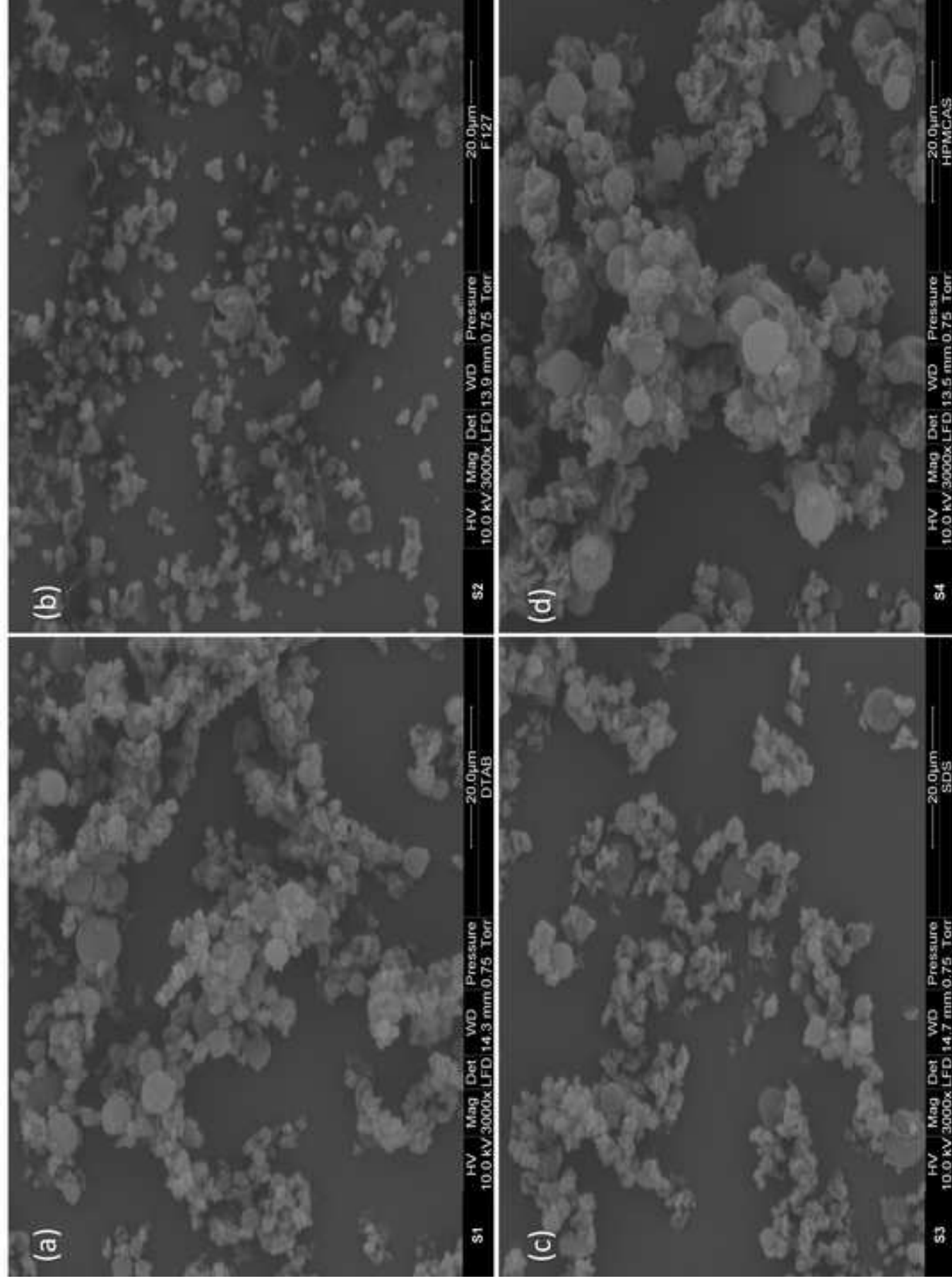


Table 1: Mass ratios (expressed as w/w%) of GF, HPMCAS and surfactant (SDS, DTAB or F127) that were used to prepare the physical mixtures.

Surfactant	GF	HPMCAS	Surfactant	GF	HPMCAS	Surfactant	GF	HPMCAS	Surfactant	GF	HPMCAS
0	10	90	1	9.5	89.5	2.5	8.75	88.75	5	7.5	87.5
0	20	80	1	19.5	79.5	2.5	18.75	78.75	5	17.5	77.5
0	30	70	1	29.5	69.5	2.5	28.75	68.75	5	27.5	67.5
0	40	60	1	39.5	59.5	2.5	38.75	58.75	5	37.5	57.5
0	50	50	1	49.5	49.5	2.5	48.75	48.75	5	47.5	47.5
0	60	40	1	59.5	39.5	2.5	58.75	38.75	5	57.5	37.5
0	70	30	1	69.5	29.5	2.5	68.75	28.75	5	67.5	27.5
0	80	20	1	79.5	19.5	2.5	78.75	18.75	5	77.5	17.5
0	90	10	1	89.5	9.5	2.5	88.75	8.75	5	87.5	7.5

Table 2: Residual solvent content measured using thermogravimetric analysis (TGA) of spray dried amorphous solid dispersions prepared using GF:HPMCAS (50%:50%) with 5% surfactant.

Surfactant added	Physical Mixture	Spray Dried Solid Dispersion
No added surfactant	1.1%	1.4 %
5% SDS	1%	0.9%
5% PF-127	0.9%	0.9%
5% DTAB	0.8%	1%